ORIGINAL REPORT: EPIDEMIOLOGIC RESEARCH

Transcriptome-wide Gene Expression Analysis in Peri-implantitis Reveals Candidate Cellular Pathways

A. Martin[1], P. Zhou[1], B.B. Singh[2], and G.A. Kotsakis[1]

Abstract: ***Objective:*** *Peri-implantitis is a condition resulting in destructive inflammation in the peri-implant soft tissue barrier. Clinically, it demonstrates vast clinical differences to periodontitis that suggest distinct inflammatory mechanisms. Implant-derived titanium particles (i-TiPs) frequently found around diseased implants appear to alter the microenvironment and confer resistance to antibiotic treatments. Studies in orthopedic implants have demonstrated potent inflammatory responses to i-TiPs involving a variety of cell types in aseptic conditions. Nonetheless, the genetic programs of cells surveilling and supporting the peri-implant soft tissue barrier in response to the combined challenges of biomaterial degradation products and oral bacteria are poorly defined. Thus, we studied gene expression specific to oral peri-implant inflammatory disease.*

Methods: *Peri-implant tissues were collected from healthy or diseased implants (*N = 10*) according to the 2018 classification criteria. Following RNA extraction and purification, a gene-level view of the transcriptome was obtained via a next-generation transcriptome-wide microarray profiling workflow (Clariom S; Applied Biosystems) that covers >20,000 well-annotated genes. A discovery analysis assessed global differential expression of genes and identified pathways in peri-implant health versus disease.*

Results: *Genes involved in the endosomal-lysosomal pathway, such as actin polymerization, were strongly upregulated in diseased tissues (*P < .05*), proposing increased intracellular activities in response to bacteria and i-TiPs. Cellular respiration pathways involved in oxidative stress were highly transcribed in all peri-implant samples, suggesting that implant-specific factors may trigger a constant state of oxidative stress.*

Conclusion: *Within the limitations of this discovery study, expressive upregulation of genes in the endosomal-lysosomal and oxidative stress pathway suggests that inflammation related to receptor-driven responses to extracellular signals, such as i-TiPs and pathogens, may have a crucial role in peri-implantitis. Results warrant external replication in validation cohorts.*

Knowledge Transfer Statement: *Our findings regarding physiologic processes affected by peri-implantitis could advance knowledge of the mechanisms and consequences of the disease. Understanding the cellular programs that partake in peri-implant inflammation has the potential to translate to novel treatment strategies for patients with peri-implantitis.*

Keywords: titanium, phagocytosis, oxidative stress, inflammation, dental implant, peri-implantitis

Introduction

Peri-implantitis has become a growing concern in the dental community because of the lack of effective treatment

DOI: 10.1177/23800844211045297. [1]Translational Periodontal Research Lab, Department of Periodontics, School of Dentistry, UT Health San Antonio, San Antonio, TX, USA; [2]Singh Lab, Department of Periodontics, School of Dentistry, UT Health San Antonio, San Antonio, TX, USA. Corresponding author: G.A. Kotsakis, UT Health San Antonio, 7703 Floyd Curl Drive, Periodontics Box, San Antonio, TX 78229, USA. Email: kotsakis@uthscsa.edu

A supplemental appendix to this article is available online.

strategies (Fretwurst et al. 2018). While peri-implantitis etiology was previously considered akin to periodontitis, distinct clinical differences between the entities suggest the need to study peri-implantitis as a distinct condition (Kotsakis and Olmedo 2021). Three key clinical observations suggest that peri-implantitis is very dissimilar to periodontitis and is affected by implant biomaterial–related factors. First, the bone destruction in peri-implantitis is more rampant than observed in periodontitis and exhibits site-specific localization and self-containment around the affected implant (Monje et al. 2019). This finding suggests that implant surface–related factors may be associated with high spatial specificity. Second, observational human studies have consistently reported implant-derived titanium particles (i-TiPs) as being significantly increased in the peri-implant microenvironment in disease versus health (Olmedo et al. 2013; Safioti et al. 2017; Fretwurst et al. 2018;). Third, mechanical and pharmacologic antimicrobial interventions that are highly effective against periodontitis have limited efficacy against peri-implantitis, with a systematic review reporting up to 100% disease relapse after 1 y for these antimicrobial treatments (Charalampakis et al. 2012; Esposito et al. 2012). This lack of efficacy of antimicrobial treatments supports a leading role of persistent i-TiPs in peri-implantitis.

While the tissue-bacterial interface in natural teeth has evolved to respond to pathogen-associated molecular patterns in microbes (Moutsopoulos and Madianos 2006), the presence of dental implants and their surface material interactions alters the natural environment. Consequently, it is not surprising that i-TiPs pose an environmental risk factor for peri-implantitis (Fretwurst et al. 2018; Wheelis et al. 2018; Daubert et al. 2019). i-TiP interactions with host tissue cells have been characterized in the context of orthopedic biomedical implants (Landgraeber et al. 2014; Grosse et al. 2015; Wright et al. 2017). Many cell types, including keratinocytes, fibroblasts, and macrophages, have demonstrated proinflammatory responses to i-TiPs (Landgraeber et al. 2014; Wright et al. 2017; Fretwurst et al. 2018). In fact, the terms "metallosis" and "metal-induced synovitis" have been introduced in the orthopedic literature to describe deposition of metallic debris into the periprosthetic soft tissues—specifically, massive release of cytokines from inflammatory cells and advanced osteolysis in the periprosthetic tissues, respectively (Romesburg et al. 2010; St Pierre et al. 2010). However, the majority of this information is based on aseptic conditions—such as those found around orthopedic implants, including metal-induced synovitis (Romesburg et al. 2010) and aseptic screw loosening—which hampers its translation to dental implants due to the ubiquitous presence of bacteria in the oral cavity.

The genetic programs of cells surveilling and maintaining the peri-implant soft tissue barrier in response to the combined challenges of biomaterial degradation products and oral bacteria are poorly defined. There is a critical need to obtain a context-specific understanding of peri-implant inflammation and determine how targeting certain cellular activities may contribute to disease prevention or therapy. The current investigation addresses this gap in knowledge by performing a differential gene expression analysis of transcriptomic responses of the soft tissue barrier in peri-implant dysbiosis versus health.

Methods

Sample Collection and RNA Extraction

We employed deidentified peri-implant tissue samples collected from otherwise healthy dental outpatients with a diagnosis of either peri-implantitis or peri-implant health in our institutional review board–approved periodontal biospecimen laboratory. Samples were collected from persons presenting for surgical procedures around healthy implants (peri-implant "healthy" group) or for peri-implantitis treatment (peri-implant "disease" group). Peri-implantitis was defined according to the 2018 classification of peri-implant diseases and conditions as sites with probing depths exceeding 6 mm, bleeding on probing, and at least 2 mm of bone loss as compared with the postloading baseline reference condition. Healthy samples were obtained from procedures such as tissue excision for contour site development around healed implant provisional restorations, as long as they included all components of the peri-implant soft tissue barrier—that is, outer and sulcular epithelia and connective tissue. Diseased samples were obtained during peri-implantitis surgical therapy, with care to obtain the entire peri-implant soft tissue barrier. Immediately after harvesting, the samples were trimmed to 2 × 3–mm dimensions and stored in RNAlater solution (Invitrogen) at −20 °C in the biospecimen repository of the Translational Periodontal Research Lab, UT Health San Antonio. gDNA was eliminated, and RNA was extracted from samples with a RNeasy Plus Mini Kit (Qiagen) according to the manufacturer's instruction, treated with proteinase K digestion, and purified via a spin column with silica gel particles. High-quality RNA samples were confirmed by measuring A260/A280 and A260/A230 ratios. To ensure an adequate proportion of full-length RNA, 2 tests were employed: 1) microfluidic analysis was used to assess RNA integrity with an Agilent 2100 Bioanalyzer; 2) 28S and 18S rRNA bands were visualized by running agarose gel electrophoresis, showing transcript size based on ribosome interactions. Upon assessment of purified RNA quantity at a threshold of 200 ng/µL, samples of appropriate quality and integrity had their gene expression profiles determined.

Gene Expression Analysis

To measure gene-level expression across the transcriptome, the Clariom S Microarray (ThermoFisher Scientific) was employed. This gene-focused array used probes tiled through the most constitutively shared exons across all

known transcripts for a given gene. The expected coverage exceeds >20,000 well-annotated human genes with detection of only constitutive exons within each gene. Isolated and purified RNA samples were submitted to the Microarray Research Services Laboratory (Affymetrix) where samples were quality control tested for RNA quality and integrity (proportion of full-length transcripts). Upon completion of these quality control assessments, 7 of the original 10 RNA samples passed all metrics and were analyzed with a Clariom S Assay as previously described (Baus-Domínguez et al. 2019; Shimura et al. 2021): 3 collected from healthy peri-implant tissue and 4 from diseased tissue. Briefly, RNA was amplified and hybridized, and the analysis was performed according to a routine protocol with the GeneChip Fluidics Station 450 (Baus-Domínguez et al. 2019).

Annotated reads of microarray data were loaded in the Transcriptome Analysis Console (Affymetrix) with the Summarization Signal Space Transformation–Robust Multichip Analysis algorithm. Samples were examined for quality control with target prep controls, a group of previously characterized polyadenylated RNA transcripts not found in eukaryotic samples, which were used to calibrate and assess the process of target preparation. Hybridization controls, a set of nonspecific labeled transcripts with increasing signal values added to hybridization data, were used to ensure proper hybridization of tested samples. Processed microarray data were then analyzed to determine any condition-specific changes in expression of select genes. The samples were analyzed by expression levels (determined by probe intensity) of all genes present. Threshold values initially used to determine significant differences between samples were a P value <0.05 and a fold change >2 or <–2. The attribute used for comparison was diseased state (diseased vs. healthy). Because this was a discovery cohort of a limited sample size, no false discovery rate adjustments were performed to maximize discovery. After determination of expression differences in the Transcriptome Analysis Console, each gene with significantly different expression was investigated with UniProt, an online functional database. This provided additional information to aid in characterizing the function of each implicated protein to suggest the types of pathways showing variation among individuals. Furthermore, the homogeneity of results was assessed across samples and by disease state with reference to the expression of the housekeeping genes glyceraldehyde 3-phosphate dehydrogenase (*GAPDH*) and β-actin and via principal component analysis, respectively.

Details were gathered about background and function of each gene to determine the processes that might function differently between the conditions. Additionally, genes were filtered by highest expression values regardless of the degree of differences between conditions. Similar analyses of P values, fold change, and protein details for the most highly expressed genes were conducted to examine the most prominent pathways in these tissues. A larger cluster of genes with the most upregulation in diseased samples was identified by use of a search filter of fold change >1.5 and $P < 0.05$ as an expanded secondary analysis; when the discovery threshold was reduced, clear mention was made in the results to highlight an increased risk for false-positive detection. Similarly, several genes with the most upregulation in healthy samples were determined by the same process but with a fold change <–1.5. Exact significance of differences and protein functions were analyzed to give clues to the types of processes that are most affected by patient condition.

Results

Processes Related to Peri-implant Inflammatory Disease

The analyzed samples were comparable for main demographic variables, such as mean ± SD patient age (healthy vs. diseased: 56.5 ± 14 vs. 61.8 ± 8 y) and sex (2 females/1 male vs. 2 females/2 males). Furthermore, implant years in function were comparable between healthy samples (5.3 ± 3 y) and diseased (6.5 ± 2 y). All samples were obtained from nonsmoking persons. We identified a panel of genes with the expressive differences (fold change >2 and $P < 0.05$) between health and disease to pinpoint the types of proteins that are most affected by a diseased state (Fig. 1). Because no genes surpassed the significance threshold for upregulation in favor of the healthy peri-implant tissue state, additional genes showing a smaller magnitude of differential upregulation were surveyed (fold change <–1.5 and $P < 0.05$) to provide an overview of functions possibly linked with homeostatic mechanisms. Due to a reduction of the fold change threshold, this analysis has a greater likelihood of producing false positives. Each gene was grouped by the type of physiologic pathway in which it is involved (Table). The most commonly implicated processes were receptor-mediated cell signaling, neural regulation and differentiation, immune responses, and the cell cycle. This suggests that a variety of homeostatic functions seem to be more transcribed in healthy tissue.

As shown in Figures 1 and 2, genes encoding proteins BLOC1S4 ($P = 0.012$), CDK12 ($P = 0.002$), WASH1 ($P = 0.021$), and DNAJC28 ($P = 0.031$) were all upregulated in diseased samples. One upregulated gene, *WASH1*, elucidates the importance of actin polymerization in disease. WASH1 serves as a nuclease-promoting factor at endosomal surfaces and induces actin polymerization for endosome sorting within the cell (Derivery et al. 2009). The actin-polymerization activity of WASH1 is through Arp2/3 complex–dependent actin assembly and participates in phagosome acidification and maturation with potentially great relevance to peri-implantitis because oral bacteria and i-TiPs accumulate in intracellular phagosomes (Taira et al. 2012). BLOC1S4

Figure 1. Plotting of expression value differences of individual genes between healthy and diseased samples. (**A**) Scatter plot of expression levels in all detectable genes between healthy and diseased samples. Each dot represents expression of a single gene. Proximity to the left y-axis and top x-axis indicates upregulation of a gene in diseased versus healthy samples and vice versa for proximity to the right y-axis and bottom x-axis. Highlighted in red are 4 genes that showed significant upregulation in disease (*BLOC1S4*, *CDK12*, *WASH1*, and *DNAJC28*). (**B**) Volcano plot shows the correlation between fold change and *P* value for gene expression differences between groups. Each dot represents fold change and *P* value of expression differences for a single gene. Red dots indicate specific genes that surpassed a threshold >2.0 fold change and $P < 0.05$ for differences in expression.

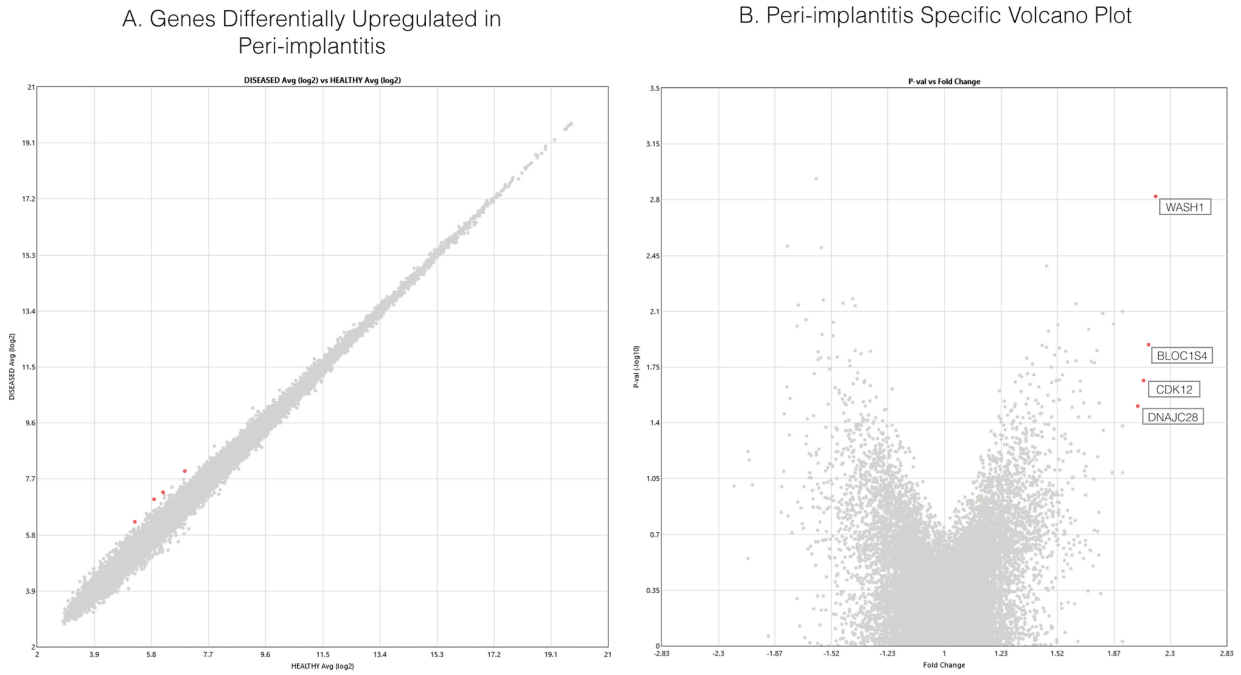

(biogenesis of lysosome-related organelles complex 1, subunit 4) was also significantly upregulated in disease, representing the same endosomal-lysosomal pathway upregulation as WASH1 (Fig. 2). The protein encoded is a subunit of BLOC-1, which plays a role in the biosynthesis of lysosomes and similar organelles and intracellular vesicle movement (Setty et al. 2007). Furthermore, CDK12 is a cyclin-dependent kinase responsible for phosphorylation of RNA polymerase II, serving as a transcriptional regulator. CDK12-mediated regulation is specific to genes involved in DNA repair and stability of the genome (Bartkowiak et al. 2010). Last, DNAJC28 is associated with canonical heat shock response (also known as *HSP40*) and seems to have a chaperone function within the Golgi apparatus, which is associated with oxidative stress (Sojourner et al. 2018). All 4 proteins seem to play some roles in intracellular vesicle formation and trafficking, oxidative stress, or transcriptional regulation of DNA maintenance genes.

Several Genes Lose Conditional Expression Differences in Absence of an Outlying Sample

To control for any superficial gene expression effects due to outlying values, we performed a principal component analysis on all 7 samples (Fig. 3). An outlying patient sample was identified; thus, sensitivity analyses were conducted by including and excluding the outlying sample to assess the dependency of expression differences on the presence of this sample. Specifically, principal component analysis found that while the majority of healthy and diseased samples remained close to the top variance determinants, 1 diseased sample showed a different transcriptional profile from other samples on the most variable component and had different baseline housekeeping gene expressions (Appendix Fig. 1; Fig. 3). Given that this component accounted for a large fraction of sample variation, it was apparent that this sample was largely different from the others, which may suggest different etiologic pathways driving inflammation in this individual.

To determine the impact of the outlying sample on gene expression changes, we identified the top 10 genes with the largest conditional differences, with and without exclusion of the outlier. Excluding the outlier moderated the fold difference of *WASH1*, which remained significantly different between conditions. While most genes showed a similar level of variance in both cases, *EZH2* (histone methyltransferase) and *OR4F17* (G protein–coupled receptor) showed drastically different conditional effects between analyses and became significant ($P < 0.05$ and fold change >2 | <–2) solely due to removal of the outlying value.

Table.
Top Candidate Genes Upregulated in Healthy vs. Diseased Tissue.

Gene Name	Function	Expression in Tissue		Fold Change
		Healthy	Diseased	
CROCC	Ciliary basal body organization; mitosis	9.46	8.77	–1.62
SNX33	Cytoskeleton; vesicle trafficking, required for mitosis	8.19	7.58	–1.53
CCNA1[a]	Regulates beginning of cell cycle in preparation for mitosis; mainly involved in meiotic differentiation	6.16	5.33	–1.78*
C11orf85	Associates telomere with inner nucleus membrane; homologous pairing during meiosis	5.83	5.14	–1.61
PLCE1[b]	Regulates small GTPases; role in cell growth/survival; function in T cells; function in kidneys	6.09	5.31	–1.72*
LYL1[a]	Transcriptional regulation; hemopoiesis/B-cell development	5.46	4.78	–1.6*
IL3RA	IL-3 receptor; cytokine signaling	5.31	4.65	–1.58
DEFB104A; DEFB104B	Antimicrobial activity; innate immune response; chemotaxis	5.48	4.63	–1.8
PTPRO	Tyrosine phosphatase activity; regulates glomerular function in kidneys; role in neural development	6.25	5.58	–1.59
IGSF11[a]	Stimulates cell growth; regulation of brain synapses	5.89	5.24	–1.57*
SLC6A16[b]	Ion transport; Involved in neurotransmitter activity	5.82	5.04	–1.71*
EN1	DNA binding; several brain development processes	5.41	4.82	–1.51
ADCY1[b]	Formation of cAMP; response to cellular $Ca2^{+}$ levels; role in circadian rhythm, possibly memory and learning	4.78	4.19	–1.5*
KCNB2	Voltage-gated potassium channel; involved in potassium current in brain (cortex) and smooth muscle cells	4.32	3.71	–1.53
P2RX4	ATP receptor; ligand-gated ion channel	7.5	6.77	–1.66
LRRC38	Voltage and calcium activated potassium channel; shifts voltage dependence	4.98	4.31	–1.59
OR52H1	Olfactory receptor	4.81	4.18	–1.55
SLC35F3	Could be thiamine transporter	4.56	3.95	–1.53
MOB3C MOB	Metal binding; could regulate kinase activity	8.03	7.19	–1.79
DNMT3A[b]	DNA methylation patterns; maternal/ paternal imprinting	7.79	7.15	–1.56*
AGPAT4[b]	Phospholipid biosynthesis pathway enzyme	7.22	6.57	–1.57
PGR	Association with MRG (involved in tumor regulation); unknown function	5.97	5.15	–1.77
ZNF135[b]	Possibly transcriptional regulation; regulates cell morphology and cytoskeletal arrangement	5.76	5.03	–1.66*
FCHO1	Involved in endocytosis; recruits clathrin-related proteins	5.7	4.97	–1.66
NOS3	Nitric oxide production; involved in vascular relaxation; angiogenesis in coronary vessels; promotes clotting	5.59	4.77	–1.76
FILIP1[b]	Regulates antiangiogenic activity in endothelial cells; inhibits melanoma growth	5.06	4.46	–1.51

Mitosis/meiosis/cell cycle
Immune responses
Neural regulation/differentiation
Receptors/ion channels
Other cellular functions

The table shows 26 genes determined to have significantly higher expression in healthy samples versus diseased samples. The filter criteria for this determination of significance were a fold change <–1.5 and a *P* value <0.05. Each row shows the gene name, a brief description of function, and expression value in healthy and diseased samples. Per the legend, rows are colored by type of process in which the gene is involved. The top 3 and top 10 most differentially expressed genes are notated. Genes were determined to be in the top 3 or top 10 by *P* values. Genes involved in immune responses, neural regulation/differentiation, and other cellular functions seemed to show the most differential expression out of represented genes. This table is available in color online.

[a]Top 3 most differentially expressed genes.

[b]Top 10 most differentially expressed genes.

*$P < 0.01$ (all fold change values, $P < 0.05$).

Figure 2. Comparison of expression levels of genes with significantly different expression across all samples and pathways implicated by upregulated genes. (**A**) Hierarchical clustering chart comparing expression levels of identified genes among the 7 tested samples. The top of the chart signifies relatedness of individual samples, with bottom groups showing the highest degree of similarity and top groups showing less similarity. Blue indicates downregulation of gene expression as compared with other genes and across samples, while red indicates upregulation. (**B**) Diagram shows the function of 3 identified genes, *WASH1*, *BLOC1S4*, and *DNAJC28*, in regulating actin polymerization, endosomal processing, and inflammation in response to titanium stimulation in macrophages. WASH1 is one of a complexes of proteins guiding the Arp 2/3 complex to the appropriate site on F-actin, where it can begin nucleation. BLOC1S4 serves to promote maturation of early endosomes into late endosomes for subsequent lysosome fusion. DNAJC28 maintains a role in vesicle formation in the Golgi apparatus and inflammasome-mediated inflammation.

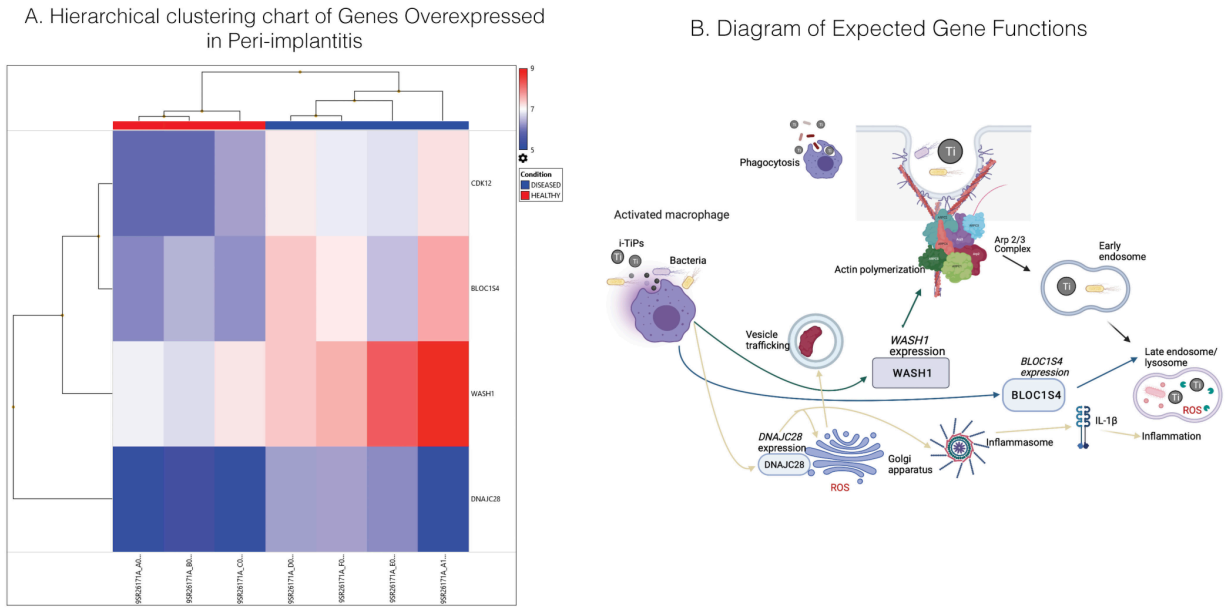

Highest-Expressing Genes Involved in Keratinization, Inflammation, and Oxidative Stress across Conditions

To develop a better understanding of the types of constitutive genes and thus the most influential pathways that are expressed in these tissues, we ranked the top 20 most highly expressed genes in health and disease. Each of these genes, apart from *SPRR2A* in diseased and *KRT6C* in healthy, were identical between conditions as suggested by the very similar heat maps ranked by disease (Fig. 4a) or health (Fig. 4b). Notably, SPRR2A and KRT6C perform similar functions in the keratinization process. This illustrates that many components of the most prominent tissue-specific processes are constitutive around implants despite inflammatory levels. Expression levels of all genes were very similar across patients and conditions, aside from an outlying sample showing downregulation of several genes, which may reveal distinct etiologies driving peri-implant inflammation. By assessment of expression differences between conditions of the most highly expressed genes, it is apparent that none of these genes show considerable contrast in expression levels. Differences among these constitutive genes are negligible. Genes involved in cellular respiration, immune function, keratinization, and other cellular functions are most represented in the top expressors. Thus, local immunity, keratinization of cells, and responses to various types of oxidative stress appear to be among the most important maintenance processes for these tissues.

Discussion

A detailed understanding of changes in cellular functions in peri-implantitis requires knowledge of the pathways implicated in peri-implant tissue pathology. To obtain this knowledge, we analyzed the gene programming of peri-implant soft tissue samples from a group of healthy patients and those with peri-implant disease. We identified gene expression differences between groups that pinpoint molecules and processes that may be responsible for the inflammation and bone degradation related to the endosomal-lysosomal pathway. Existing transcriptomics studies have pointed to altered gene expression pathways related to extracellular matrix molecules (Roediger et al. 2009), matrix-degrading enzymes (Roediger et al. 2009; Cho et al. 2020), and inflammatory pathways such as the cyclooxygenase 2 pathway (Liu et al. 2020) and the RANKL/OPG pathway (Becker et al. 2014; Liu et al. 2020). Importantly, when Becker et al. (2014) compared genome-wide transcriptome profiles of 7 patients with peri-implantitis versus 7 with periodontitis, they observed drastic

Figure 3. Analysis of variability and effects on genes that are most differentially expressed between conditions caused by an outlying sample. (**A**) Three-dimensional principal component analysis (PCA) charts examining overall variance among 3 major sources across samples. The PCA1 axis represents sample differences related to the most distinguishing variance source. PCA2 and PCA3 represent differences across the next largest sources of variation. Blue indicates a healthy sample, while red indicates a diseased sample. (Top panel) Chart assessing overall variance from major determinants among all samples, including the outlier. (Bottom panel) Chart depicting variance among samples with the exclusion of the outlying sample. (**B**) Charts displaying gene names and compared *P* values and fold changes between the scenarios (outlier inclusion vs. exclusion) for the 10 most significantly different genes when assessed (top) with and (bottom) without the outlying sample. Colors indicate the amount of change in expression of a particular gene between scenarios, with red being the most severely affected genes and green representing the least affected.

A. PCA for assessment of homogeneity in transcriptional responses

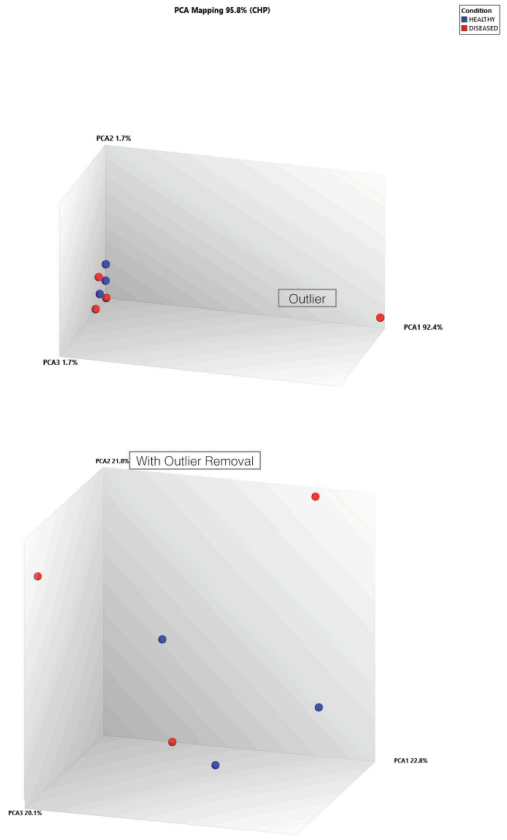

B. Top-10 Differentially Expressed Genes

10 Most Significantly Different Genes without outlier exclusion:

	Including outlier		Not including outlier	
Gene Name	**p- value**	**Fold change**	**p-value**	**Fold change**
CDK12	0.0015	2.17	0.0004	1.81
TCEB2	0.0080	1.92	0.0007	1.75
PAIP2	0.0082	1.79	0.8203	-1.02
EPS15L1	0.0096	1.86	0.0073	1.34
BLOC1S4	0.0129	2.12	0.0021	1.81
WASH1	0.0216	2.08	0.0367	1.28
DNAJC28	0.0312	2.04	0.0003	1.96
DEFB104A	0.0350	-1.80	0.0245	-1.87
SCAI	0.0415	1.92	0.0030	1.83
LACTB2	0.0445	1.8	0.0081	1.43

10 Most Significantly Different Genes with outlier exclusion:

	Not including outlier		Including outlier	
Gene Name	**p- value**	**Fold change**	**p-value**	**Fold change**
DNAJC28	0.0003	1.96	0.0312	2.04
DPH7	0.0014	-1.92	0.8700	-1.91
FOXM1	0.0015	1.94	0.1898	1.56
TAGAP	0.0037	1.96	0.9385	1.92
SLC38A7	0.0040	1.93	0.1042	1.31
EZH2	0.0056	-2.2	0.3655	-1.13
OR4F17	0.0117	2.26	0.0386	1.4
COLQ	0.0186	-1.94	0.1355	-1.36
TBX10	0.0264	-2.14	0.1011	-1.46
SAR1B	0.0275	2.3	0.2259	1.58

Close in both scenarios
Genes with >0.05 p-value difference OR >0.4 fold change difference
Genes with >0.20 p-value difference OR >0.8 fold change difference

differences in the types of pathways that were most prevalent in each condition. In peri-implant tissues, the regulation of transcripts related to innate immune responses and defense responses was dominating, while in periodontitis tissues bacterial response systems prevailed (Becker et al. 2014). In corroboration, a recent whole exome sequencing pilot study performed gene cluster enrichment analysis in 6 patients with severe peri-implantitis and found that metal ion binding was located in the center of all clusters, indicating that dysfunction of regulation in metal ion concentration might affect cellular activities related to implant failure (Lee et al. 2014). These results are highly concordant with our findings of endosomal-lysosomal and oxidative stress pathway involvement, which has been shown to be the main pathway activated during i-TiP phagocytosis (Taira et al. 2012). Nonetheless, bacterial system response genes were not upregulated in peri-implant disease versus health in our study.

Consideration of the combination of these factors supports the biological plausibility of i-TiPs contributing to bacterial-driven inflammation and peri-implant dysbiosis. This hypothesis is consistent with the challenges to reverse peri-implantitis with existing antimicrobial treatment strategies. In this study, we found several genes implicated in intracellular vesicle trafficking to be upregulated in peri-implant disease as compared with healthy controls. One upregulated gene, *WASH1*, illuminated the presence of an overexpressed Arp2/3 complex–mediated actin polymerization pathway. Other upregulated genes, *BLOC1S4* and *DNAJC28*, emphasized the importance of endosomal formation

Figure 4. Comparison of expression and functions of the 20 most highly expressed genes between healthy and diseased samples. (**A**, **B**) Hierarchical clustering charts compare expression levels of the most highly expressed genes in healthy and diseased samples. Blue indicates a downregulation of gene expression as compared with other genes and across samples, while red indicates upregulation. Charts comparing expression levels of the most highly expressed genes in (A) diseased and (B) healthy samples. (**C**) Diagram depicts abbreviated names and expression values of the 20 most abundant genes in chronological order in health (left) and disease (right). Arrows show the location of each gene in relation to that gene in the other condition. Dashed arrows indicate genes that are lower in order in diseased versus healthy samples. Per the legend, colors show the type of physiologic function that the highlighted gene is involved in.

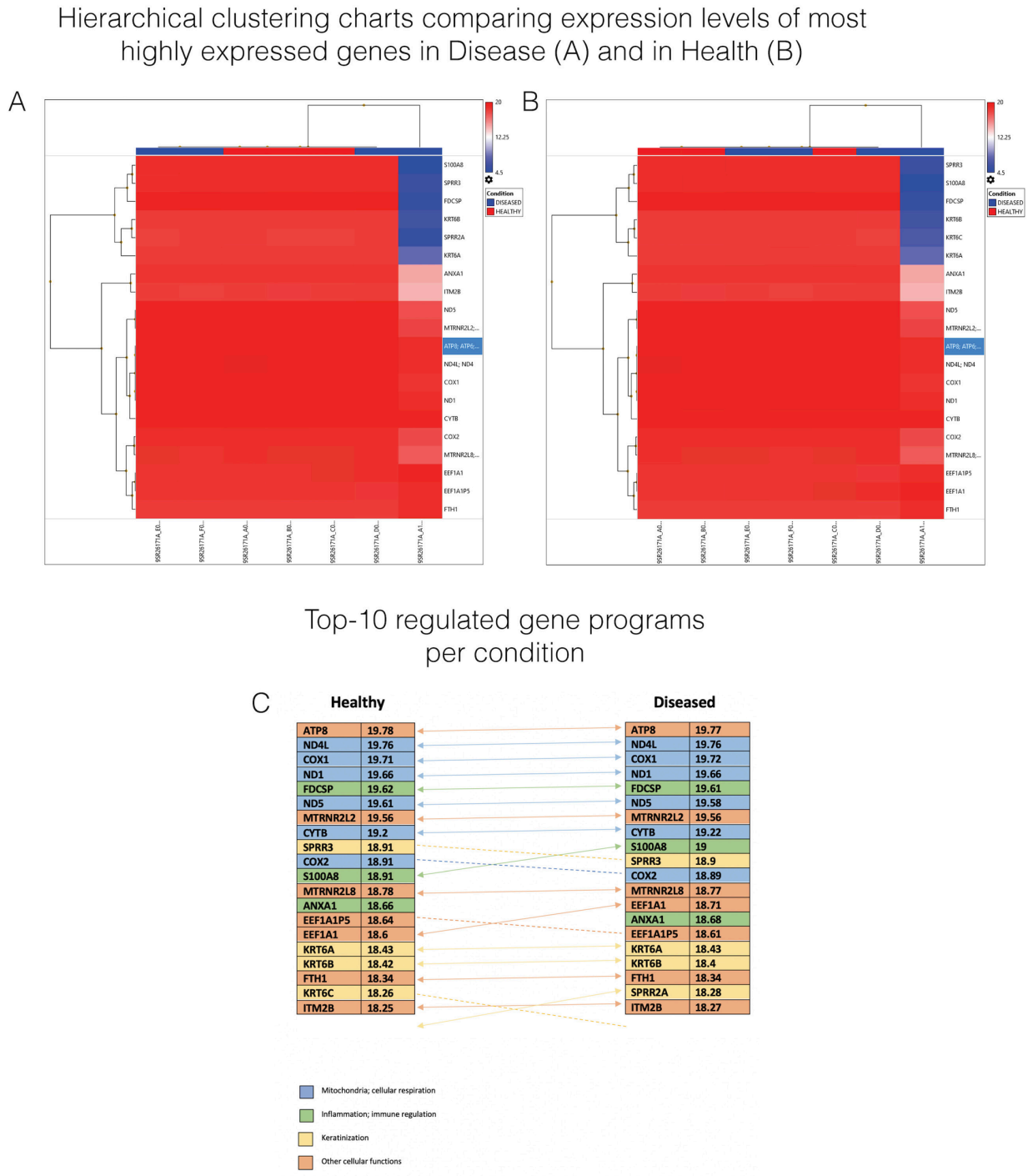

and trafficking. Differential expression of genes involved in endosomal processing and actin polymerization suggests that peri-implantitis is associated with increased actin activity and overall intracellular trafficking around the implant site, likely contributing to an inflammatory response. Because bacteria and i-TiPs require similar membrane internalization events, it is not possible to disaggregate differences due to endocytosis and intracellular processing of i-TiPs in peri-implant disease. One study comparing transcriptome expression patterns between peri-implantitis and periodontitis showed that certain genes involved in actin regulation, endosomal processing, and antigen presentation are expressed differently between the groups, furthering the idea that upregulation of these processes may be unique to peri-implantitis (Roediger et al. 2009). These findings are crucial because some compounds (CK-666, CK-869) have been shown to inhibit Arp2/3 actin nucleation activity in vitro and thus potentially function to reduce inflammation and other pathology instigated by i-TiPs in peri-implantitis (Hetrick et al. 2013).

Upon investigation of several of the most upregulated transcripts in healthy samples, genes related to a variety of physiologic processes were identified. Implicated physiologic pathways included cell cycle, immune system responses, neural activity, cell signaling, and other processes. Peri-implantitis may affect the integrity of many body systems, rather than just local epithelia. It appears to dampen cell cycle function, mucosal immunity, and neural processes in affected tissues. Consistent with genetic studies of periodontitis (Marchesan 2020), several proinflammatory cytokine genes thought to be important in peri-implantitis, such as IL-1b, did not show significantly differential expression between conditions. This is likely due to other inflammation-related genes playing a more dominant role in immune responses in peri-implantitis. Alternatively, the possibility exists that because posttranslational modifications are critical in the role of IL-1β through inflammasomes, differences in disease versus health can be found farther upstream in the expression of regulatory molecules. Downregulation of genes involved in immunity could be caused by damaging Ti interactions with immune cells and result in an impaired immune response. Reduced neural activity could suggest defective neurologic functions in oral tissues in response to damage inflicted by i-TiPs, but this requires further study. Regarding the most highly expressed genes in tissue samples overall, genes involved in keratinization, inflammation, and oxidative stress responses were most abundant across healthy and diseased tissues. Keratin production, oxidative burst, and inflammation appear to play constitutive roles in oral tissue surrounding implants. This indicates that a high baseline level of inflammation and oxidative stress is expected in this tissue, regardless of patient condition. Notably, 1 diseased sample presented a strikingly different genetic profile overall. While many genes identified as having differential expression between health and disease lost significance in the absence of the outlying sample, the pathways most implicated in expression differences were unaffected. Our findings regarding modulation of a variety of molecular processes in peri-implantitis have the potential to advance the field of peri-implant therapy by identifying and interrogating the cellular physiology most relevant to the disease.

Despite providing substantial data related to cellular physiology involved in peri-implantitis, this study has limitations. Most notably, because of the high RNA input requirements for the interrogation of a vast number of genes in this transcriptome-wide discovery analysis, only 7 samples were included. Thus, obtained analyses were not adjusted for multiple testing, which may have inflated type I error. As such, this discovery study requires independent validation studies. Additionally, the lack of direct quantification of titanium content in the tissues makes it challenging to directly associate the implication of i-TiPs with increased phagocytosis pathway activation or identify whether the outlying sample may stem from a different etiology of peri-implantitis in certain patients, such as that driven by bacteria or titanium particles bacterial-driven versus titanium particle-driven. Future prospective studies with rigorous phenotyping of each case and with assessment of various candidate etiopathologic agents for peri-implantitis are required to enable patient stratification and determination of etiology-driven gene expression changes in peri-implantitis tissues.

Author Contributions

A. Martin, contributed to data analysis, drafted the manuscript; P. Zhou, B.B. Singh, contributed to data interpretation, critically revised the manuscript; G.A. Kotsakis, contributed to conception, design, data acquisition, analysis, and interpretation, drafted the manuscript. All authors gave final approval and agree to be accountable for all aspects of the work.

Declaration of Conflicting Interests

The authors declared no potential conflicts of interest with respect to the research, authorship, and/or publication of this article.

Funding

The authors disclosed receipt of the following financial support for the research, authorship, and/or publication of this article: National Institutes of Health / National Institute of Dental and Craniofacial Research R03 DE029872 awarded to G.A. Kotsakis.

Ethical Approval

Tissue samples were collected from discarded surgical tissue and stored in the periodontics tissue repository that had been approved by the research ethics board at UT Health San Antonio.

Data Sharing and Transparency

Data of the study are publicly available at https://www.ncbi.nlm.nih.gov/geo/query/acc.cgi?acc=GSE178351.

References

Bartkowiak B, Liu P, Phatnani HP, Fuda NJ, Cooper JJ, Price DH, Adelman K, Lis JT, Greenleaf AL. 2010. Cdk12 is a transcription elongation-associated CTD kinase, the metazoan ortholog of yeast Ctk1. Genes Dev. 24(20):2303–2316.

Baus-Domínguez M, Gómez-Díaz R, Torres-Lagares D, Corcuera-Flores JR, Ruiz-Villandiego JC, Machuca-Portillo G, Gutiérrez-Pérez JL, Serrera-Figallo MA. 2019. Differential expression of inflammation-related genes in down syndrome patients with or without periodontal disease. Mediators Inflamm. 2019:4567106.

Becker ST, Beck-Broichsitter BE, Graetz C, Dorfer CE, Wiltfang J, Hasler R. 2014. Peri-implantitis versus periodontitis: functional differences indicated by transcriptome profiling. Clin Implant Dent Relat Res. 16(3):401–411.

Charalampakis G, Leonhardt A, Rabe P, Dahlen G. 2012. Clinical and microbiological characteristics of peri-implantitis cases: a retrospective multicentre study. Clin Oral Implants Res. 23(9):1045–1054.

Cho YD, Kim PJ, Kim HG, Seol YJ, Lee YM, Ryoo HM, Ku Y. 2020. Transcriptome and methylome analysis of periodontitis and peri-implantitis with tobacco use. Gene. 727:144258.

Daubert DM, Pozhitkov AE, Safioti LM, Kotsakis GA. 2019. Association of global DNA methylation to titanium and peri-implantitis: a case-control study. JDR Clin Trans Res. 4(3):284–291.

Derivery E, Sousa C, Gautier JJ, Lombard B, Loew D, Gautreau A. 2009. The Arp2/3 activator wash controls the fission of endosomes through a large multiprotein complex. Dev Cell. 17(5):712–723.

Esposito M, Grusovin MG, Worthington HV. 2012. Interventions for replacing missing teeth: treatment of peri-implantitis. Cochrane Database Syst Rev. 1:CD004970.

Fretwurst T, Nelson K, Tarnow DP, Wang HL, Giannobile WV. 2018. Is metal particle release associated with peri-implant bone destruction? An emerging concept. J Dent Res. 97(3):259–265.

Grosse S, Haugland HK, Lilleng P, Ellison P, Hallan G, Hol PJ. 2015. Wear particles and ions from cemented and uncemented titanium-based hip prostheses—a histological and chemical analysis of retrieval material. J Biomed Mater Res B Appl Biomater. 103(3):709–717.

Hetrick B, Han MS, Helgeson LA, Nolen BJ. 2013. Small molecules CK-666 and CK-869 inhibit actin-related protein 2/3 complex by blocking an activating conformational change. Chem Biol. 20(5):701–712.

Kotsakis GA, Olmedo DG. 2021. Peri-implantitis is not periodontitis: scientific discoveries shed light on microbiome-biomaterial interactions that may determine disease phenotype. Periodontol 2000. 86(1):231–240.

Landgraeber S, Jager M, Jacobs JJ, Hallab NJ. 2014. The pathology of orthopedic implant failure is mediated by innate immune system cytokines. Mediators Inflamm. 2014:185150.

Lee S, Kim JY, Hwang J, Kim S, Lee JH, Han DH. 2014. Investigation of pathogenic genes in peri-implantitis from implant clustering failure patients: a whole-exome sequencing pilot study. PloS One. 9(6):e99360.

Liu Y, Liu Q, Li Z, Acharya A, Chen D, Chen Z, Mattheos N, Chen Z, Huang B. 2020. Long non-coding RNA and mRNA expression profiles in peri-implantitis vs periodontitis. J Periodontal Res. 55(3):342–353.

Marchesan JT. 2020. Inflammasomes as contributors to periodontal disease. J Periodontol. 91 Suppl 1:S6–S11.

Monje A, Pons R, Insua A, Nart J, Wang HL, Schwarz F. 2019. Morphology and severity of peri-implantitis bone defects. Clin Implant Dent Relat Res. 21(4):635–643.

Moutsopoulos NM, Madianos PN. 2006. Low-grade inflammation in chronic infectious diseases: paradigm of periodontal infections. Ann N Y Acad Sci. 1088:251–264.

Olmedo DG, Nalli G, Verdu S, Paparella ML, Cabrini RL. 2013. Exfoliative cytology and titanium dental implants: a pilot study. J Periodontol. 84(1):78–83.

Roediger M, Miró X, Geffers R, Irmer M, Huels A, Miosge N, Gersdorff N. 2009. Profiling of differentially expressed genes in peri-implantitis and periodontitis in vivo by microarray analysis. J Oral Biosci. 51(1):31–45.

Romesburg JW, Wasserman PL, Schoppe CH. 2010. Metallosis and metal-induced synovitis following total knee arthroplasty: review of radiographic and CT findings. J Radiol Case Rep. 4(9):7–17.

Safioti LM, Kotsakis GA, Pozhitkov AE, Chung WO, Daubert DM. 2017. Increased levels of dissolved titanium are associated with peri-implantitis—a cross-sectional study. J Periodontol. 88(5):436–442.

Setty SR, Tenza D, Truschel ST, Chou E, Sviderskaya EV, Theos AC, Lamoreux ML, Di Pietro SM, Starcevic M, Bennett DC, et al. 2007. Bloc-1 is required for cargo-specific sorting from vacuolar early endosomes toward lysosome-related organelles. Mol Biol Cell. 18(3):768–780.

Shimura T, Sharma P, Sharma GG, Banwait JK, Goel A. 2021. Enhanced anti-cancer activity of andrographis with oligomeric proanthocyanidins through activation of metabolic and ferroptosis pathways in colorectal cancer. Sci Rep. 11(1):7548.

Sojourner SJ, Graham WM, Whitmore AM, Miles JS, Freeny D, Flores-Rozas H. 2018. The role of HSP40 conserved motifs in the response to cytotoxic stress. J Nat Sci. 4(4):e500.

St Pierre CA, Chan M, Iwakura Y, Ayers DC, Kurt-Jones EA, Finberg RW. 2010. Periprosthetic osteolysis: characterizing the innate immune response to titanium wear-particles. J Orthop Res. 28(11):1418–1424.

Taira M, Sasaki M, Kimura S. 2012. Macrophage reaction against sub-micron titanium particles. In: Sasaki K, Suzuki O, Takahashi N, editors. Interface oral health science 2011. Tokyo: Springer. p. 283–284.

Wheelis SE, Montano-Figueroa AG, Quevedo-Lopez M, Rodrigues DC. 2018. Effects of titanium oxide surface properties on bone-forming and soft tissue-forming cells. Clin Implant Dent Relat Res. 20(5):838–847.

Wright C, Iyer AK, Wang L, Wu N, Yakisich JS, Rojanasakul Y, Azad N. 2017. Effects of titanium dioxide nanoparticles on human keratinocytes. Drug Chem Toxicol. 40(1):90–100.